Generation of Gravitational Waves due to Magnetohydrodynamic Turbulence in the Early Universe

PhD Final Examination

Alberto Roper Pol (PhD candidate)

Faculty Advisor: Brian Argrow

Research Advisor: Axel Brandenburg

Collaborators: Tina Kahniashvili, Arthur Kosowsky & Sayan Mandal

University of Colorado at Boulder

Laboratory for Atmospheric and Space Physics (LASP)

May 8, 2020

Laboratory for Atmospheric and Space Physics
University of Colorado **Boulder**

A. Roper Pol *et al., Geophys. Astrophys. Fluid Dyn.* **114**, 130. arXiv:1807.05479 (2020)

A. Roper Pol *et al., submitted to Phys. Rev. D* arXiv:1903.08585 (2020)

Overview

Introduction and Motivation

- Generation of cosmological gravitational waves (GWs) during phase transitions and inflation
  - **Electroweak phase transition** ~ 100 GeV
  - Quantum chromodynamic (QCD) phase transition ~ 100 MeV
  - Inflation

Introduction and Motivation

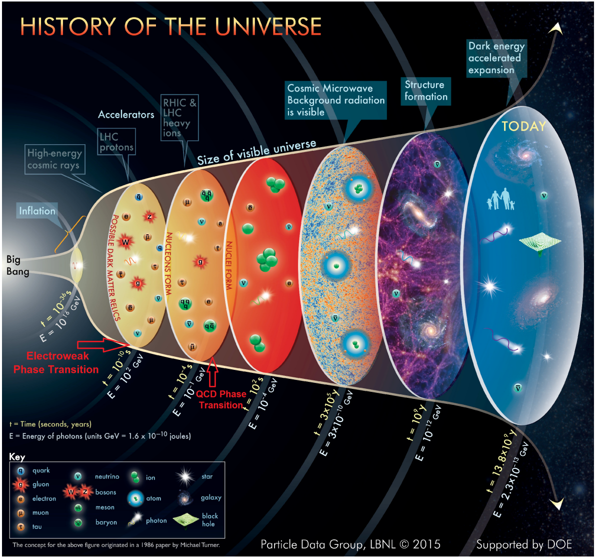

Introduction and Motivation

- Generation of cosmological gravitational waves (GWs) during phase transitions and inflation
  - Electroweak phase transition ~ 100 GeV
  - Quantum chromodynamic (QCD) phase transition ~ 100 MeV
  - Inflation
- GW radiation as a probe of early universe physics
- Possibility of GWs detection with
  - **Space-based GW detector LISA**
  - Pulsar Timing Arrays (PTA)
  - B-mode of CMB polarization

Introduction and Motivation

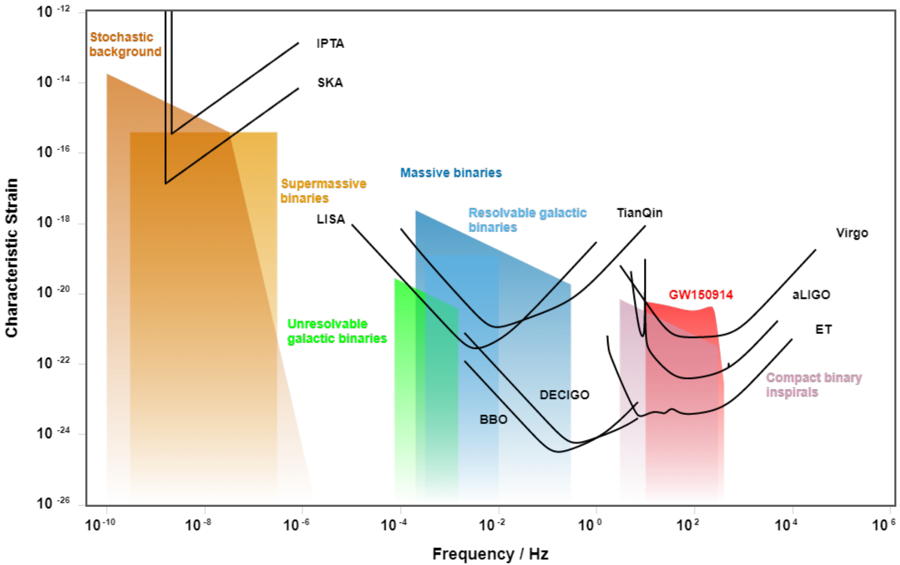

Introduction and Motivation

LISA

- Laser Interferometer Space Antenna (LISA) is a space–based GW detector
- LISA is planned for 2034
- LISA was approved in 2017 as one of the main research missions of ESA
- LISA is composed by three spacecrafts in a distance of 2.5M km

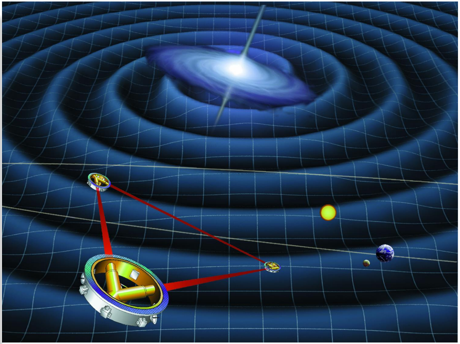

Figure: Artist's impression of LISA from Wikipedia

Orbit of LISA

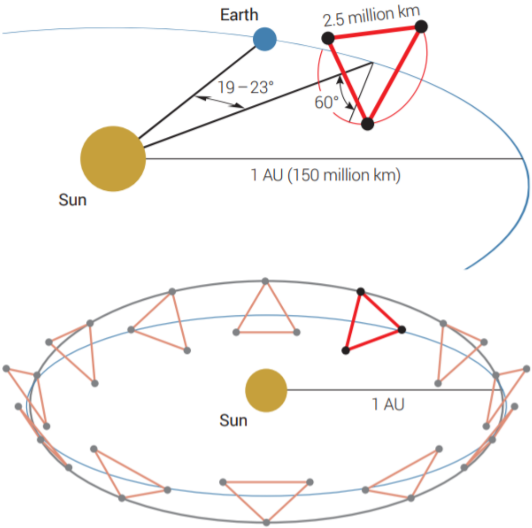

Introduction and Motivation

- Generation of cosmological gravitational waves (GWs) during phase transitions and inflation
  - Electroweak phase transition ~ 100 GeV
  - Quantum chromodynamic (QCD) phase transition ~ 100 MeV
  - Inflation
- GW radiation as a probe of early universe physics
- Possibility of GWs detection with
  - Space-based GW detector LISA
  - Pulsar Timing Arrays (PTA)
  - B-mode of CMB polarization
- Magnetohydrodynamic (MHD) sources of GWs:
  - Hydrodynamic turbulence from phase transition bubbles nucleation
  - Primordial magnetic fields
- Numerical simulations using PENCIL CODE to solve:
  - Relativistic MHD equations
  - Gravitational waves equation

Evidence of primordial magnetic fields

There are different astrophysical evidences that indicate the presence of a large scale coherent magnetic field.[1]

Fermi blazar observations

- Gamma rays from blazars ($\sim$1 TeV) interact with extragalactic background light
- Generation of electron - positron beam
- Observed power removal from gamma-ray beam

[1] L. M. Widrow
Rev. of Mod. Phys., **74** 775–823 (2002)

Evidence of primordial magnetic fields

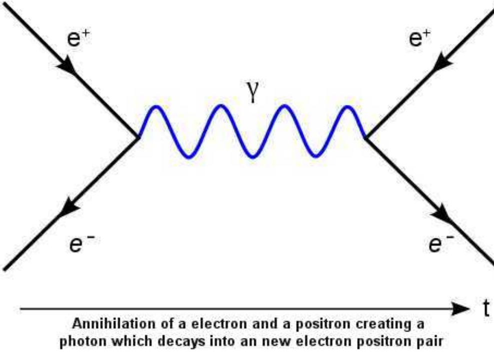

Evidence of primordial magnetic fields

Solution

- Large scale (intergalactic) magnetic fields could deviate the electron-positron from beam in opposite directions
- Recombination does not happen leading to lose of energy
- Strength $\sim 10^{-16}$ G, scale ~ 100 kpc[2]

Origin

Intergalactic magnetic fields could have been originated from:

- Astrophysical or
- Cosmological seed fields

subsequently amplified during structure formation

[2] A. M. Taylor, I. Vovk, and A. Neronov *Astron. & Astrophys.*, **529** A144, (2011)

Evidence of primordial magnetic fields

Helicity

- Magnetic helicity is observed in present astrophysical objects
- Fractional magnetic helicity is required in cosmological seed fields
- Primordial helical magnetic fields require a first order phase transition:
    - Electroweak phase transition (EWPT) $t \sim 10^{-12}$ s
    - Quantum chromodynamics (QCD) phase transtion $t \sim 10^{-6}$ s

Definition (Magnetic Helicity)

$$\mathcal{H} = \left\langle \boldsymbol{B} \cdot (\nabla \times)^{-1} \boldsymbol{B} \right\rangle = \langle \boldsymbol{A} \cdot \boldsymbol{B} \rangle$$

MHD description

Right after the electroweak phase transition we can model the plasma using continuum MHD

- Quark-gluon plasma
- Charge-neutral, electrically conducting fluid
- Relativistic magnetohydrodynamic (MHD) equations
- Ultrarelativistic equation of state

$$p = \rho c^2/3$$

- Friedmann–Lemaître–Robertson–Walker model

$$g_{\mu\nu} = \mathrm{diag}\{-1, a^2, a^2, a^2\}$$

Contributions to the stress-energy tensor

$$T^{\mu\nu} = \left(p/c^2 + \rho\right) U^\mu U^\nu + p g^{\mu\nu} + F^{\mu\gamma} F^{\nu}{}_{\gamma} - \frac{1}{4} g^{\mu\nu} F_{\lambda\gamma} F^{\lambda\gamma},$$

- From fluid motions
  $T_{ij} = \left(p/c^2 + \rho\right) \gamma^2 u_i u_j + p\delta_{ij}$
  Relativistic equation of state:
  $p = \rho c^2/3$
- From magnetic fields:
  $T_{ij} = -B_i B_j + \delta_{ij} B^2/2$

- 4–velocity $U^\mu = \gamma(c, u^i)$
- 4–potential $A^\mu = (\phi/c, A^i)$
- 4–current $J^\mu = (c\rho_{\rm e}, J^i)$
- Faraday tensor $F^{\mu\nu} = \partial^\mu A^\nu - \partial^\nu A^\mu$

MHD equations

Conservation laws

$$T^{\mu\nu}{}_{;\nu} = 0$$

Relativistic MHD equations are reduced to[3]

MHD equations

$$\frac{\partial \ln \rho}{\partial t} = -\frac{4}{3}\left(\nabla \cdot \boldsymbol{u} + \boldsymbol{u} \cdot \nabla \ln \rho\right) + \frac{1}{\rho c^2}\left[\boldsymbol{u} \cdot (\boldsymbol{J} \times \boldsymbol{B}) + \eta \boldsymbol{J}^2\right]$$

$$\frac{D\boldsymbol{u}}{Dt} = \frac{1}{3}\mathbf{u}\left(\nabla \cdot \boldsymbol{u} + \boldsymbol{u} \cdot \nabla \ln \rho\right) - \frac{\boldsymbol{u}}{\rho c^2}\left[\boldsymbol{u} \cdot (\boldsymbol{J} \times \boldsymbol{B}) + \eta J^2\right] - \frac{1}{4}c^2 \nabla \ln \rho + \frac{3}{4\rho}\boldsymbol{J} \times \boldsymbol{B} + \frac{2}{\rho}\nabla \cdot (\rho \nu \boldsymbol{S})$$

for a flat expanding universe with comoving and normalized $p = a^4 p_{\rm phys}, \rho = a^4 \rho_{\rm phys}, B_i = a^2 B_{i,_{\rm phys}}, u_i$, and conformal time t.

[3] A. Brandenburg, K. Enqvist, and P. Olesen, *Phys. Rev. D* **54**, 1291 (1996)

MHD equations

Electromagnetic fields are obtained from Faraday tensor as

$$\mathbf{B} = \nabla \times \mathbf{A}, \quad \mathbf{E} = -\nabla\phi - \frac{\partial \mathbf{A}}{\partial t}$$

Generalized Ohm's law

$$\mathbf{E} = \eta \mathbf{J} - \mathbf{u} \times \mathbf{B}$$

Maxwell equations

$$\nabla \cdot \mathbf{E} = \rho_{\rm e} c^2, \qquad \nabla \cdot \mathbf{B} = 0$$

$$\nabla \times \mathbf{B} = \mathbf{J} + \cancel{\frac{1}{c^2}\frac{\partial \mathbf{E}}{\partial t}} \qquad \frac{\partial \mathbf{B}}{\partial t} = -\nabla \times \mathbf{E}$$

Maxwell equations + Ohm's law combined:

$$\frac{\partial \boldsymbol{B}}{\partial t} = \boldsymbol{\nabla} \times (\boldsymbol{u} \times \boldsymbol{B} - \eta \boldsymbol{J})$$

Evolution of magnetic strength and correlation length

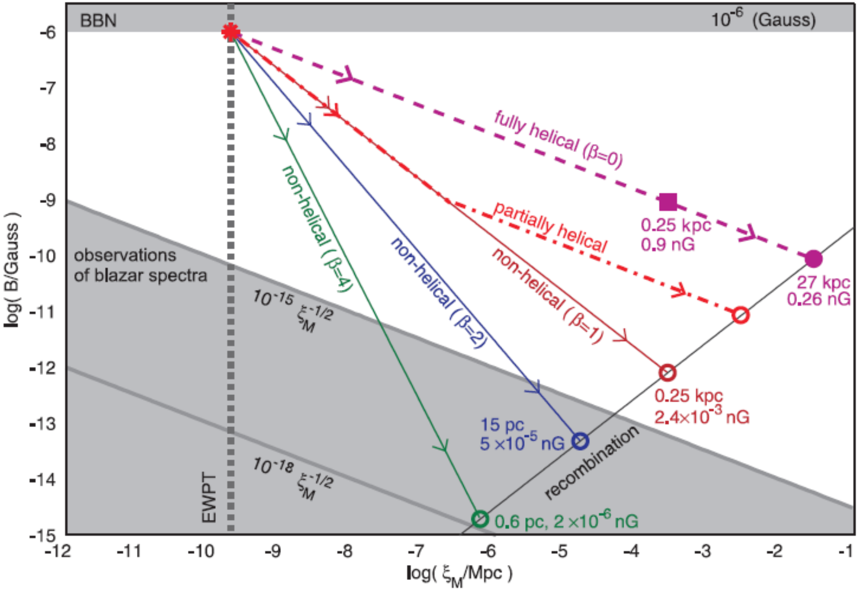

Gravitational waves equation

GWs equation for an expanding flat Universe

- Assumptions: isotropic and homogeneous Universe
- Friedmann–Lemaître–Robertson–Walker (FLRW) metric $\gamma_{ij} = a^2 \delta_{ij}$
- Tensor-mode perturbations above the FLRW model:

$$g_{ij} = a^2 \left(\delta_{ij} + h_{ij}^{\rm phys} \right)$$

- GWs equation is[4]

$$\left(\partial_t^2 - \cancel{\frac{a''}{a}} - c^2 \nabla^2 \right) h_{ij} = \frac{16\pi G}{\mathbf{a} c^2} T_{ij}^{\rm TT}$$

  - h_{ij} are rescaled $h_{ij} = a h_{ij}^{\rm phys}$
  - Comoving spatial coordinates $\nabla = a \nabla^{\rm phys}$
  - Conformal time ${\rm d}t = a \, {\rm d}t^{\rm phys}$
  - Comoving stress-energy tensor components $T_{ij} = a^4 T_{ij}^{\rm phys}$
  - Radiation-dominated epoch such that $a'' = 0$

[4] L. P. Grishchuk, *Sov. Phys. JETP*, 40, 409-415 (1974)

Normalized GW equation[5]

$$\left(\partial_t^2 - \nabla^2\right) h_{ij} = 6\, T_{ij}^{\mathrm{TT}} / t$$

Properties

- All variables are normalized and non-dimensional
- Conformal time is normalized with t_*
- Comoving coordinates are normalized with c/H_*
- Stress-energy tensor is normalized with $\mathcal{E}_{\mathrm{rad}}^* = 3H_*^2 c^2/(8\pi G)$
- Scale factor is $a_* = 1$, such that $a = t$

[5] A. Roper Pol *et al.*, *Geophys. Astrophys. Fluid Dyn.* **114**, 130. arXiv:1807.05479 (2020)

Gravitational waves equation

Properties

- Tensor-mode perturbations are gauge invariant
- h_{ij} has only two degrees of freedom: h^+, $h^\times$
- The metric tensor is traceless and transverse (TT gauge)

Linear polarization modes $+$ and $\times$

Linear polarization basis (defined in Fourier space)

$$e_{ij}^{+} = (\boldsymbol{e}_1 \times \boldsymbol{e}_1 - \boldsymbol{e}_2 \times \boldsymbol{e}_2)_{ij}$$

$$e_{ij}^{\times} = (\boldsymbol{e}_1 \times \boldsymbol{e}_2 + \boldsymbol{e}_2 \times \boldsymbol{e}_1)_{ij}$$

Orthogonality property

$e_{ij}^{A} e_{ij}^{B} = 2\delta_{AB}$, where $A, B = +, \times$

$+$ and $\times$ modes

$$\tilde{h}^{+} = \frac{1}{2} e_{ij}^{+} \tilde{h}_{ij}^{\mathrm{TT}}, \qquad \tilde{T}^{+} = \frac{1}{2} e_{ij}^{+} \tilde{T}_{ij}^{\mathrm{TT}}$$

$$\tilde{h}^{\times} = \frac{1}{2} e_{ij}^{\times} \tilde{h}_{ij}^{\mathrm{TT}}, \qquad \tilde{T}^{\times} = \frac{1}{2} e_{ij}^{\times} \tilde{T}_{ij}^{\mathrm{TT}}$$

Numerical considerations

- CFL condition for stability:

$$\delta_t \leq C_{\rm CFL} \delta x / U_{\rm eff},$$

$$U_{\rm eff} = |\boldsymbol{u}| + (c_{\rm s}^2 + v_{\rm A}^2)^{1/2},\ c_{\rm s}^2 = c^2/3,\ v_{\rm A}^2 = B^2/\rho.$$

- Projection of $T_{ij}^{\rm TT}$ requires non-local Fourier transform $\tilde{T}_{ij}$:

$$\tilde{T}_{ij}^{\rm TT} = \left(P_{il} P_{jm} - \frac{1}{2} P_{ij} P_{lm} \right) \tilde{T}_{lm}$$

where $P_{ij} = \delta_{ij} - \hat{k}_i \hat{k}_j$

Method 1

- Solve the GWs equation sourced by the stress-energy tensor[6]

$$\left(\partial_t^2 - \nabla^2\right) h_{ij} = 6\, T_{ij}/t$$

- Evolution of 6 components in physical space
- Project h_{ij}^{TT} only when we are interested in spectra

$$\tilde{h}_{ij}^{\mathrm{TT}} = \left(P_{il} P_{jm} - \frac{1}{2} P_{ij} P_{lm}\right) \tilde{h}_{lm}$$

- Compute $\tilde{h}^{+}$, $\tilde{h}^{\times}$ modes

[6] A. Roper Pol *et al.*, *Geophys. Astrophys. Fluid Dyn.* **114**, 130. arXiv:1807.05479 (2020)

GWs energy density:

$$\Omega_{\rm GW}(t) = \mathcal{E}_{\rm GW}/\mathcal{E}^*_{\rm rad}, \quad \mathcal{E}^*_{\rm rad} = \frac{3H_*^2c^2}{8\pi G}$$

$$\Omega_{\rm GW}(t) = \int_{-\infty}^{\infty} \Omega_{\rm GW}(k,t)\,{\rm d}\ln k$$

$$\boldsymbol{\Omega}_{\rm GW}(\mathbf{k},\mathbf{t}) = \frac{k}{6H_*^2}\int_{4\pi}\left(\left|\dot{\tilde{h}}_+^{\rm phys}\right|^2 + \left|\dot{\tilde{h}}_\times^{\rm phys}\right|^2\right)k^2\,{\rm d}\Omega_k$$

Magnetic/kinetic energy density:

$$\Omega_{\rm M,K}(t) = \int_{-\infty}^{\infty} \Omega_{\rm M,K}(k,t)\,{\rm d}\ln k$$

$$\boldsymbol{\Omega}_{\rm M}(\mathbf{k},\mathbf{t}) = \frac{k}{2}\int_{4\pi}\left(\tilde{\mathbf{B}}\cdot\tilde{\mathbf{B}}^*\right)k^2\,{\rm d}\Omega_k, \quad \boldsymbol{\Omega}_{\rm K}(\mathbf{k},\mathbf{t}) = \frac{k}{2}\int_{4\pi}\rho\,(\tilde{\mathbf{u}}\cdot\tilde{\mathbf{u}}^*)\,k^2\,{\rm d}\Omega_k$$

Numerical accuracy[7]

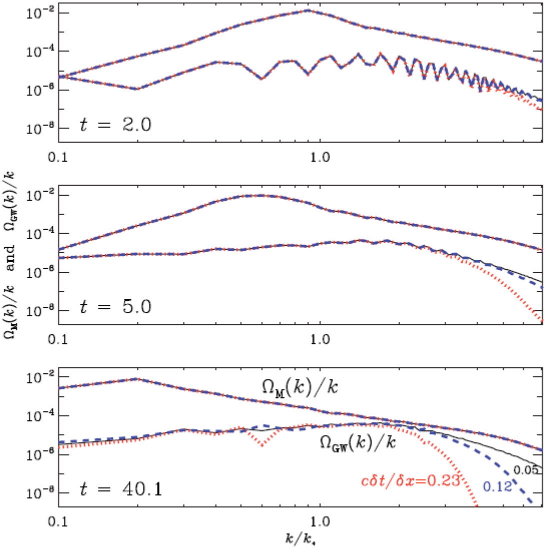

- CFL condition is not enough for GW solution to be numerically accurate
- $c\delta t/\delta x \sim 0.05 \ll 1$
- Higher resolution is required
- Hydromagnetic turbulence does not seem to be affected

[7] A. Roper Pol *et al., Geophys. Astrophys. Fluid Dyn.* **114**, 130. arXiv:1807.05479 (2020)

Method 2

- Compute Fourier transform of stress-energy tensor $\tilde{T}_{ij}$
- Project into TT gauge $\tilde{T}_{ij}^{\mathrm{TT}} = \left(P_{il} P_{jm} - \frac{1}{2} P_{ij} P_{lm}\right) \tilde{T}_{lm}^{\mathrm{TT}}$
- Compute $\tilde{T}^{+}$ and $\tilde{T}^{\times}$ modes
- Discretize time using δt from MHD simulations (CFL condition)
- Assume $\tilde{T}^{+,\times}/t$ to be constant between subsequent timesteps (robust as $\delta t \to 0$)
- GW equation solved analytically between subsequent timesteps in Fourier space[8]

$$\begin{pmatrix} \omega \tilde{h} - 6\omega^{-1} \tilde{T}/t \\ \tilde{h}' \end{pmatrix}_{+,\times}^{t+\delta t} = \begin{pmatrix} \cos \omega \delta t & \sin \omega \delta t \\ -\sin \omega \delta t & \cos \omega \delta t \end{pmatrix} \begin{pmatrix} \omega \tilde{h} - 6\omega^{-1} \tilde{T}/t \\ \tilde{h}' \end{pmatrix}_{+,\times}^{t}$$

[8] A. Roper Pol *et al.*, *Geophys. Astrophys. Fluid Dyn.*, **114**, 130 arXiv:1807.05479 (2020)

Frequency of oscillations of GWs vs MHD waves

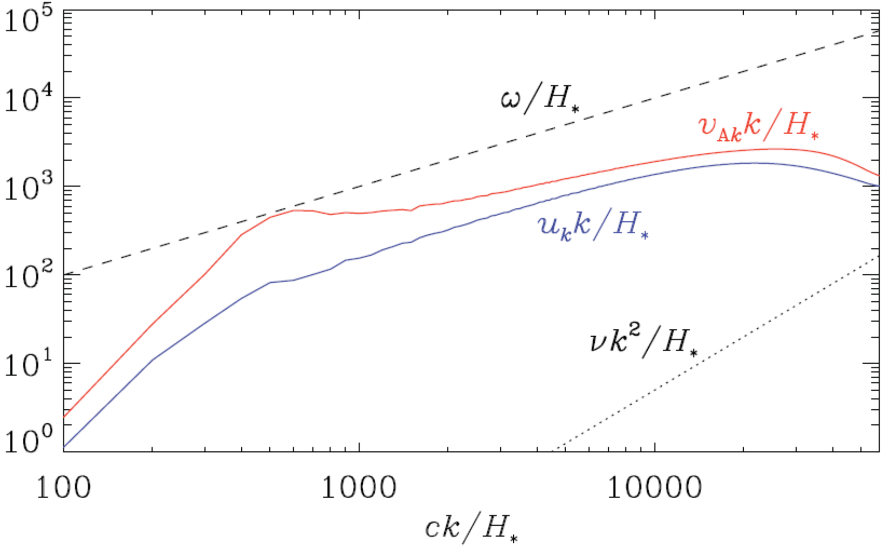

Numerical results for decaying MHD turbulence[9]

Initial conditions

- Fully helical stochastic magnetic field
- Batchelor spectrum, i.e., $E_{\rm M} \propto k^4$ for small k
- Kolmogorov spectrum for inertial range, i.e., $E_{\rm M} \propto k^{-5/3}$
- Total energy density at t_* is $\sim 10\%$ to the radiation energy density
- Spectral peak at $k_{\rm M} = 100 \cdot 2\pi$, normalized with $k_H = 1/(cH)$

Numerical parameters

- 1152^3 mesh gridpoints
- 1152 processors
- Wall-clock time of runs is $\sim 1-5$ days

[9] A. Brandenburg, *et al.* *Phys. Rev. D* **96**, 123528 (2017), A. Roper Pol, *et al.* arXiv:1903.08585 (2020)

Initial magnetic spectra

$$k_{\rm M} = 15$$

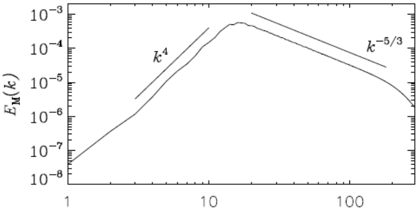

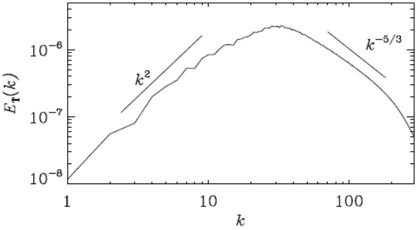

$$E_{\rm M}(k) = \frac{1}{2} \int_{4\pi} \left(\tilde{\mathbf{B}}(k) \cdot \tilde{\mathbf{B}}^*(k) \right) k^2 d\Omega$$

$$\Omega_{\rm M} = \int_0^\infty E_{\rm M}(k) dk$$

$$E_{\rm T}(k) = \int_{4\pi} \left(\tilde{\mathbf{T}}_{ij}(k) \tilde{\mathbf{T}}_{ij}^*(k) \right) k^2 d\Omega$$

$$E_{\rm T}(k) = \frac{1}{2} \int_{4\pi} \left(\tilde{\mathbf{B}}^2(k) \tilde{\mathbf{B}}^{2,*}(k) \right) k^2 d\Omega$$

$$\Omega_{\rm T} = \int_0^\infty E_{\rm T}(k) dk$$

Numerical results for decaying MHD turbulence

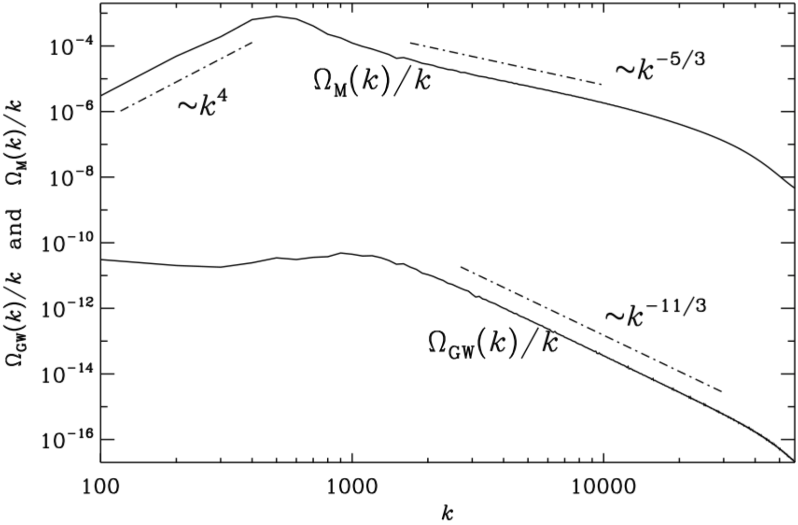

Comments

- **Novel k^0 scaling in the subinertial range**

Polarization degree

- Helical magnetic fields induce circularly polarized GWs
- Helicity and GWs polarization have same sign
- Agreement with analytical prediction[10]
- Illustrated with a 1D Beltrami field example

[10] T. Kahniashvili *et al.*, *Phys. Rev. Lett.*, **95** (15):151301 (2005)

1D Beltrami field

- Magnetic field: $\boldsymbol{B}(x) = B_0\,(0, \sin k_0 x, \cos k_0 x)$, such that $\boldsymbol{B} \cdot (\boldsymbol{\nabla} \times \boldsymbol{B}) = \mathrm{sgn}\,(k_0)$
- Stress-energy tensor: $T_{ij} = \frac{1}{2} B_0^2 \begin{pmatrix} 0 & 0 & 0 \\ 0 & -\cos 2k_0 x & \sin 2k_0 x \\ 0 & \sin 2k_0 x & \cos 2k_0 x \end{pmatrix}$

  which is already TT with two independent modes:

$$T^+ = -\frac{1}{2} B_0^2 \cos 2k_0 x, \quad T^\times = -\frac{1}{2} B_0^2 \sin 2k_0 x$$

- Tensor-mode perturbations:

$$h^+(x,t) = -\frac{2\pi G}{c^4 k_0^2} B_0^2 \cos 2k_0 x (1 - \cos 2k_0 ct)$$

$$h^\times(x,t) = -\frac{2\pi G}{c^4 k_0^2} B_0^2 \sin 2k_0 x (1 - \cos 2k_0 ct)$$

Early time evolution of GW energy density spectral slope

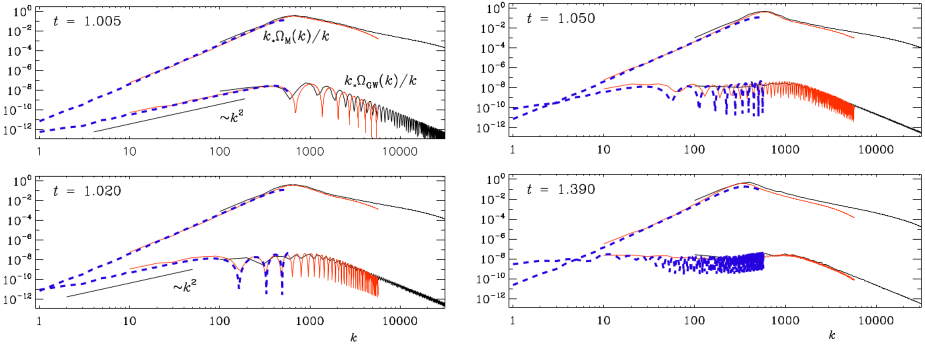

Signal at the present time

Characteristic amplitude of GWs

$$h_{\rm c}^2(t) = \int_{-\infty}^{\infty} h_{\rm c}^2(k,t)\, {\rm d} \ln k, \quad \mathbf{h_{\rm c}^2(k,t)} = \int_{4\pi} \left(\left|\tilde{h}_+^{\rm phys}\right|^2 + \left|\tilde{h}_\times^{\rm phys}\right|^2 \right) k^2 \, {\rm d}\Omega_k$$

GW energy density and characteristic amplitude

- Shifting due to the expansion of the universe:
  - $\Omega_{\rm GW}^0(k) = a_0^{-4} (H_*/H_0)^2 \Omega_{\rm GW}(k, t_{\rm end})$
  - $h_{\rm c}^0(k) = a_0^{-1} h_{\rm c}(k, t_{\rm end})$
  - $f = a_0^{-1} H_* k/(2\pi)$

$$a_0 \approx 1.254 \cdot 10^{15} \, (T_*/100 \text{ GeV}) \, (g_{\rm S}/100)$$

$$H_* \approx 2.066 \cdot 10^{-11} \text{ s}^{-1} \, (T_*/100 \text{ GeV})^2 \, (g_*/100)^{1/2}$$

$$H_0 = 100 h_0 \text{ kms}^{-1} \text{ Mpc}^{-1}$$

Numerical results for decaying MHD turbulence

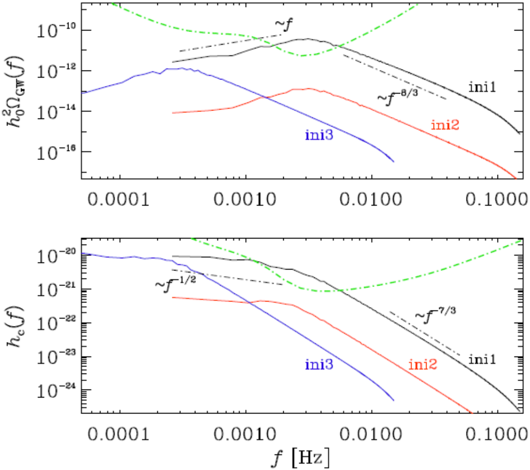

Run	$\mathcal{E}_0, \mathcal{F}_0$	η	$\Omega_i^{\rm max}$	$\Omega_{\rm GW}^{\rm sat}$	i	hel	$t_{\rm max}$	N
ini1	—	5e-6	1.16e-01	2.05e-09	M	y	1.00	100
ini2	—	5e-8	7.62e-03	6.38e-12	M	y	1.00	100
ini3	—	5e-7	7.62e-03	6.36e-10	M	y	1.00	10

Time evolution of GW energy density

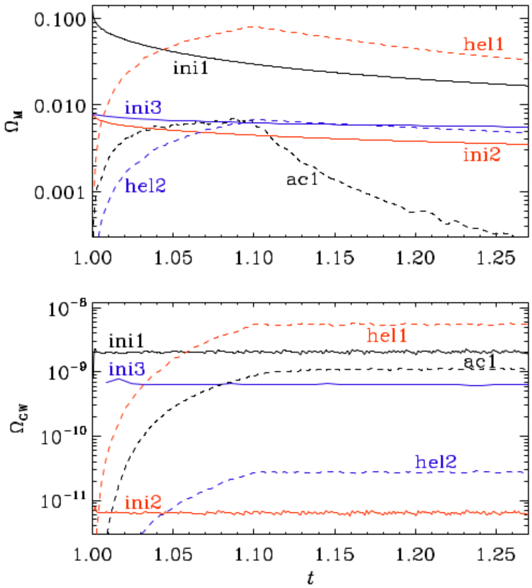

Forced turbulence (built-up primordial magnetic fields and hydrodynamic turbulence)

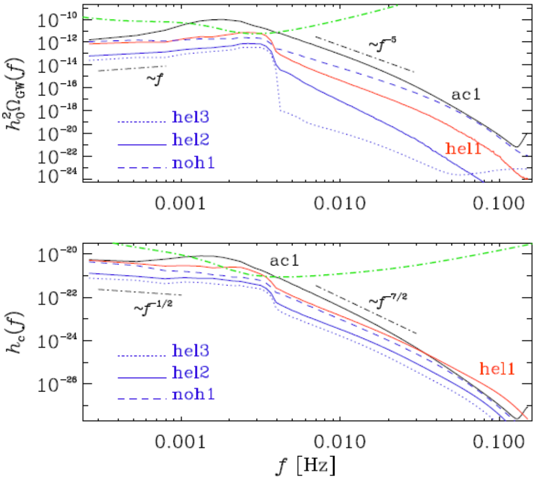

Run	$\mathcal{E}_0, \mathcal{F}_0$	η	$\Omega_i^{\max}$	$\Omega_{\rm GW}^{\rm sat}$	i	hel	$t_{\max}$	N
hel1	1.4e-3	5e-7	2.17e-02	4.43e-09	M	y	1.10	100
hel2	8.0e-4	5e-7	7.18e-03	4.67e-10	M	y	1.10	100
hel3	2.0e-3	5e-7	4.62e-03	2.09e-10	M	y	1.01	100
hel4	1.0e-4	2e-6	5.49e-03	1.10e-11	M	y	1.01	1000
noh1	1.4e-3	5e-7	1.44e-02	3.10e-09	M	n	1.10	100
noh2	8.0e-4	2e-6	4.86e-03	3.46e-10	M	n	1.10	100
ac1	3.0	2e-5	1.33e-02	5.66e-08	K	n	1.10	100
ac2	3.0	5e-5	1.00e-02	3.52e-08	K	n	1.10	100
ac3	1.0	5e-6	2.87e-03	2.75e-09	K	n	1.10	100

Forced turbulence (built-up primordial magnetic fields and hydrodynamic turbulence)

Conclusions

- Much stronger signal found for acoustic than for rotational turbulence
- Result in agreement with literature[11]
- In both cases, GWs polarization is zero
- **Novel k^0 scaling in the subinertial range**
- Smooth bump for acoustic runs around the spectral peak
- Steeper than Kolmogorov GW spectra in the inertial range

[11] M. Hindmarsh *et al.*, *Phys. Rev. D*, **92** 12:123009 (2015)

Conclusions

- We have implemented a module within the open-source PENCIL CODE that allows to obtain background stochastic GW spectra from primordial magnetic fields and hydrodynamic turbulence.
- For some of our simulations we obtain a detectable signal by future GW detector LISA.
- GW equation is normalized such that it can be easily scaled for different times within the radiation-dominated epoch.
- Novel f spectrum obtained for GWs in high frequencies range vs f^3 obtained from analytical estimates
- Bubble nucleation and magnetogenesis physics can be coupled to our equations for more realistic production analysis.

The End

Thank You!

NSF

შოთა რუსთაველის ეროვნული
სამეცნიერო ფონდი
SHOTA RUSTAVELI NATIONAL
SCIENCE FOUNDATION

LASP
Laboratory for Atmospheric and Space Physics
University of Colorado **Boulder**

NORDITA
The Nordic Institute for Theoretical Physics

HELIAE • UNIVERSITAS • PUBLICA • LIGAMUS

alberto.roperpol@colorado.edu